On the Accuracy of an Indoor Location-sensing Technique Suitable for Impulse Radio Networks

Wenyu Guo and Nick P. Filer
School of Computer Science
The University of Manchester
Oxford Road, Manchester, M13 9PL, UK
Email: {guow, nick}@cs.man.ac.uk

***Abstract*-An impulse radio indoor mapping and positioning technique has been proposed. This technique enables impulse radios to use the times of arrival (TOAs) of dominant echoes from the surrounding environment to generate a map showing the major features of the environment and pinpoint themselves on this map. This technique can be used to aid indoor applications designed for location-based services or for wireless sensor networks used in disaster zones. 2D Mapping and positioning algorithms have been developed for the proposed technique. As the timer in an impulse radio receiver cannot be exact, errors are introduced into the measured TOAs of dominant echoes. This paper uses the reconstructions of simple indoor environments, which are common substructures of indoor geometries, to show the effects of time measurement errors in reconstructed scenarios. An approach to improve the accuracy is addressed and this approach can be applied to the reconstructions of more complex scenarios.**

I. INTRODUCTION

The Global Positioning System (GPS), the dominant system offering location information outdoors, suffers a poor indoor performance due to low signal availability, as GPS signals are not designed to penetrate through most construction materials. This has recently made indoor localisation a hot research topic. Many indoor positioning techniques have been developed, most of which rely on fixed references to determine the location of tagged devices [1-5]. This architecture implies that location information is only available in environments where references with known positions have been deployed. However, in many scenarios where location information is very useful, a reference system is not likely to have been previously deployed. For example, when a fire brigade is rescuing people from a smoke-filled building, a fireman needs to know his location in order to find the nearest exit or corridor. Also, a fireman needs to know the position of his colleagues in order to help or get help from them. In this case, there is no time for the fire brigade to deploy a reference system before entering the building. Therefore, an indoor wireless system providing location information without fixed references would be useful.

In situations where a reference system is not available, mobile nodes need to locate themselves. Therefore, we have been investigating indoor location sensing using radio-equipped mobile nodes. The fine time resolution [6,7] of impulse radios makes them an ideal candidate for positioning applications indoors. A technique suitable for impulse radios to map the surrounding environment and pinpoint themselves in relation to the environment has been proposed.

A. Proposed technique

Multipath signals from the same transmitter can be treated as originated from different images of the transmitter in surrounding walls. As these images are spontaneously synchronised with the transmitter, by measuring the time differences of arrival (TDOAs) among multipath signals, a receiver can be constrained onto hyperbolae with the transmitter and its images as foci.

These images are spontaneously synchronised with the transmitters, i.e. whenever the transmitter transmits a pulse, all its images "transmit" at the same time. Using transmitters and their images in the walls as references solves the problem of synchronisation among references, which is usually very costly to implement in conventional positioning systems, e.g. the Global Positioning System equips individual satellites with atomic clocks for synchronisation purposes.

Reducing the complexity of the system is one of the most efficient methods to reduce the cost. To make the system simple, receivers are insensitive to amplitude or phase. Only times of arrival (TOAs) of echoes with energy above the receiving threshold can be detected in individual radios. It has been found in indoor multipath measurements at a range of frequencies [8,9] that received echoes comprise a small number of dominant echoes from large flat surfaces like walls, interspersed with noise-like scattering from smaller objects across the entire range of delays.

It can be expected that, by suitable thresholding in receivers, only dominant pulses including the direct line-of-sight (LOS), single reflections and most double reflections are detected. The TOAs of these dominant pulses can then be used to map the major features of the environment.

The calculations are not trivial, but they only need to be updated at a sufficient rate to update the mapping information and track the movements of radio users. This is expected to be well within the capacity of impulse radios and therefore can be done by individual users locally. Today's timer in the receiver of an impulse radio can resolve down to near 10ps time delay [10], which suggests approximately 0.3cm along-the-path spatial resolution.

B. Paper outline

This paper is organised as follows: in section II, the fundamentals of developed 2D mapping and positioning algorithms are briefly described by using the reconstructions of two very simple indoor scenarios; based on the algorithms described in section II, in section III, the effect of errors from time measurements in scenario reconstructions are discussed; at the end, conclusions are drawn in section IV.

II. ALGORITHM FUNDAMENTALS

A. Single-wall Scenario

Fig. 1 shows a scenario with two impulse radios operating in an environment consisting of a single wall. There are four channels, whose impulse responses (CIRs) are represented by $CIR_{1,1}$, $CIR_{1,2}$, $CIR_{2,1}$ and $CIR_{2,2}$, where the first subscript is the transmitter and the second is the receiver. By reciprocity, $CIR_{1,2}$ is the same as $CIR_{2,1}$.

$CIR_{2,2}$ consists of a single echo with a delay corresponding to the round-trip time to the wall and back at the speed of light. From this, we can calculate R_2's distance from the wall, or from its image on the other side of the wall. At pedestrian speeds in indoor environments (~1.5 m/s), the distance to the image cannot change by more than 3 cm in 10ms. During this period the radio can transmit up to 200,000 pulses at 20Mpulses/s, so there is plenty of scope for improving the accuracy by averaging.

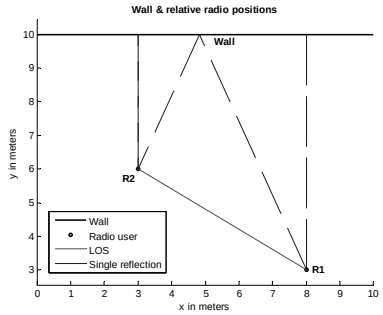

Fig. 1. Two radios communicate in a 1-wall environment

$CIR_{1,2}$ consists of two pulses, one by the LOS and the other by reflection from the wall. We cannot measure the times of flight (TOFs) of the pulses because we do not know when it was transmitted, but we can measure the time difference between the arrivals of the two pulses. This places R_1 on a hyperbola, whose foci are R_2 and its image in the wall, as shown in Fig. 2. The wall is represented by the straight line perpendicular to the line joining the foci, and half way between them.

$CIR_{1,1}$ consists of a single echo with a delay corresponding to the round-trip time from R_1 to the wall and back at the speed of light. From this we can calculate R_1's distance from the wall. This is shown by the straight line parallel to the wall, a fixed distance away from it. Where this line cuts the hyperbola is the position of R_1, relative to R_2 and the wall. Clearly there is a mirror-image ambiguity as the line cuts the hyperbola in two places, leading to two possible relative positions.

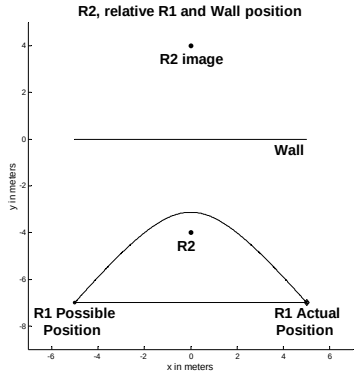

Fig. 2. Possible positions of R2 derived in relation to R1 and its image

B. Orientation Ambiguity

There is a further angular uncertainty, as we have no fixed frame of reference, so the wall could have any orientation between $\pm\ \pi$ relative to compass north. This uncertainty can be resolved by waiting until one of the radios moves, and then repeating the position calculation. We can now use the direction of motion as the reference direction, and display the wall and the other radio relative to a "track" showing the new and old positions of the moving radio, as shown in Fig. 3. The mirror-image ambiguity still remains at this stage, however.

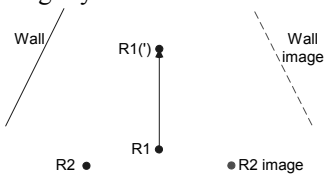

Fig. 3. Orientation ambiguity is resolved when user R1 has moved to R1('), while the mirror-image ambiguity remains

C. Two-wall Scenario

In the two-wall scenario shown in Fig. 4, the angle between the walls has been set slightly less than $\pi/2$ to clarify the effects of double reflections. $CIR_{1,1}$ contains three echoes. The first two are single reflections, one from each of the walls. The last one is the double reflection from both walls "around the corner". At this point, the system does not know that this is a double reflection, so we set up three separate coordinate systems, one for each echo, with a focal length corresponding to the three round-trip delays.

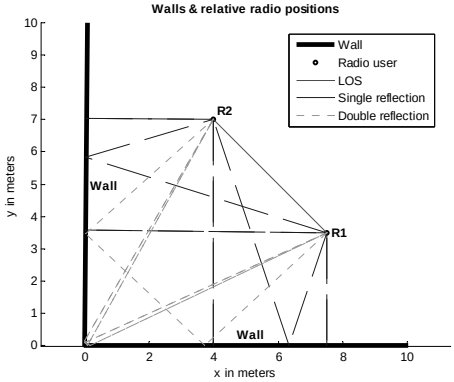

Fig. 4. Two radios communicate in a 2-wall environment

$CIR_{2,1}$ contains four pulses, one by the LOS, two by single reflections from the two walls, and one by double reflection "around the corner". Again, the system does not know that this is a double reflection, so we may create up to three hyperbolae on each of the three coordinate systems, i.e. up to nine hyperbolae in total. In the example of Fig. 5, only two hyperbolae are shown for the shortest focal length because one of the $CIR_{2,1}$ path length differences is greater than this focal length, so the third hyperbola is not "real".

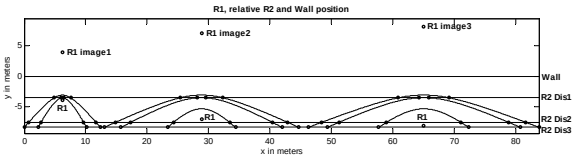

Fig. 5. Locus of R2 as hyperbolae in three separate coordinate systems

$CIR_{2,2}$ contains three echoes, two single reflections and one "around the corner" double reflection. Again, the system does not know that there are only two walls and not three, so we set up three lines cutting the hyperbolae at up to 54 positions, i.e. up to 27 pairs of mirror images.

Now the distance between the two radios is the distance from the focus to the point where the line cuts the hyperbola, and this can only take a single value. Using this knowledge we can eliminate most of the possible false scenarios. Initially, we consider the two shortest focal lengths, as these are the most likely to represent single reflections. Each of these offers up to nine possible distances between the radios, but in general only one value will appear in both sets. By placing the two foci together, and rotating one coordinate system until the second radio's positions match, we can generate four possible geometries of the surroundings, resulting from the two hyperbola cutting points in each coordinate system. The four geometries form two mirror-image pairs. Leaving the mirror-image ambiguity, two of the four geometries are shown in Fig. 6.

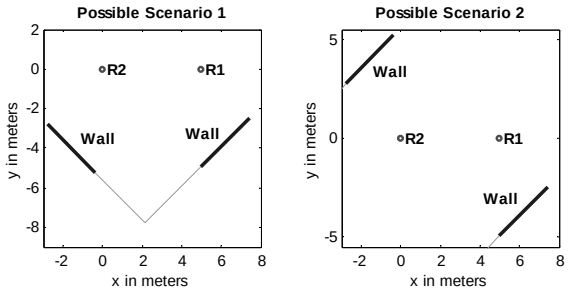

Fig. 6. Generated possible geometries of the surroundings

We now reconstruct the CIRs that would be expected from the two candidate geometries to check whether they predict double reflections that match the remaining echoes in the actual measured CIRs. If one of them does, we can identify the third focal length and coordinate system as a double reflection and eliminate it from further consideration, at the same time eliminating the other candidate geometry.

The rotational uncertainty and mirror-image ambiguity remain, but the two-wall case is now essentially solved.

D. Mirror-Image Ambiguity

The mirror-image ambiguity can be resolved when either of the radios is detected to have moved twice in different directions. By repeating the mapping process at a certain frequency that allows radio users to make detectable movements, the path of the moving radio can be represented as a "track" in relation to the surroundings. Now if the moving radio has turned left, the correct "track" will also have turned left, whereas the "track" of the mirror image will have turned right, and vice versa. If the radio user knows which way he/she has turned, the ambiguity can be resolved. If the radios are carried by robots and their control circuits can tell which way they have turned within tens of milliseconds, the mirror-image ambiguity will be resolved within this short period of time. Human users may also be expected to know which way they have turned, given a longer period of time. If the system is used to track radio tags without this intelligence, some other means of measuring rotation may be needed, e.g. accelerometers.

E. More Walls and More Radios

Where there are more than two walls, the technique is essentially the same, with multiple iterations. There will clearly be more echoes, more potential focal lengths, hyperbolae and inter-radio distances. We start by taking the two shortest focal lengths, checking whether these predict double reflections from the nearest two walls in the CIRs, and eliminating any focal lengths corresponding to these double reflections. The process is then repeated for the first and third shortest focal lengths, and echoes corresponding to double reflections from the first and third nearest walls are eliminated, and so on until we have the minimum set of walls that account for all the measured echoes in the CIRs.

Where there are more than two radios, each pair may have a different sub-set of the structures in a complex environment "in view". They will therefore be able to exchange partial maps to build up a more complete picture of a complex environment.

III. THE EFFECT OF TIMER ERRORS

The timer in an impulse radio receiver can not be exact. As a result, in a self-to-self radio channel, the round-trip delay of an echo could be measured as any value in the range of $t_{delay} \pm t_{resolution}$, where t_{delay} is the actual delay and $t_{resolution}$ is the resolution of the timer. When a measured delay is used to determine the distance from a wall, this distance will be estimated as in the range of $d_{wall} \pm \frac{t_{resolution} \times c}{2}$, where d_{wall} is the actual distance from the wall and c is the speed of light. When the radio and its image in a wall are used as the foci to set up a coordinate system, the focal length will be estimated as in the range of

$d_{fl} \pm \frac{t_{resolution} \times c}{2}$, where d_{fl} is the actual distance from the radio to its image in the wall.

A. Single-wall Scenario

In the scenario in Fig. 1, when estimating the position of radio R1 in relation to R2 and the wall by using R2 and its image in the wall as the foci, taking into account the effect of a 1ns timer resolution, estimated possible positions of R1 will be in two regions showing a mirror-image ambiguity instead of two points, as shown in Fig. 7, where the boundaries of the regions are solid lines, while the actual lines of position (LOPs) are dashed lines. The two hyperbolae in the figure take into account both the possible error in the focal length derived from the TOF of the echo in $CIR_{2,2}$ and the effect of the error in the TDOA between the LOS and the single reflection in $CIR_{1,2}$. Here, the purpose of using a very low timer resolution of 1ns instead of an achievable value of 10ps [10] is to achieve a clearer visible effect in the figure. Assuming the mirror-image ambiguity has been resolved using the method described in section II.D, an enlarged view of the region showing the actual possible positions of R1 is shown in Fig. 8.

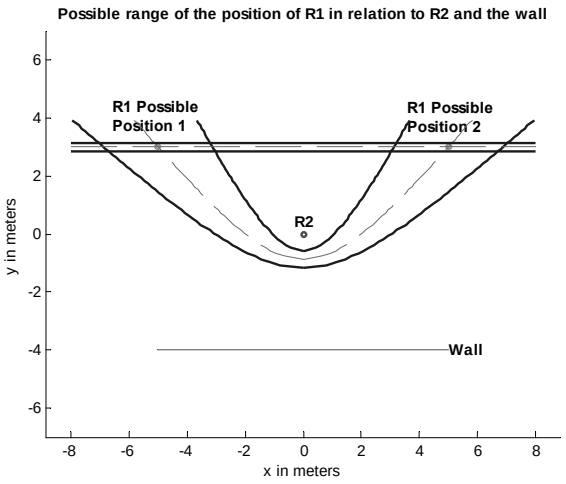

Fig. 7. Possible positions of R1 in relation to R2 and the wall after taking into account of 1ns timer error

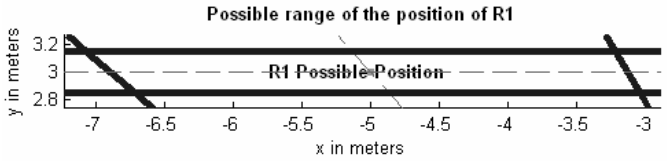

Fig. 8. Enlarged view of the region showing the actual possible positions of R1

The other way round, if R1 and its image in the wall are used as foci to estimate the position of R2 in relation to R1 and the wall, the possible positions of R2 will be in two regions showing mirror-image ambiguity as shown in Fig. 9. Assuming the mirror-image ambiguity has been resolved, an enlarged view of the region showing the actual possible positions of R2 is shown in Fig. 10.

By comparing the sizes of the regions in Fig. 8 and Fig. 10, it is found that they are similar. This suggests that using either R1 with its image in the wall or R2 with its image as references to reconstruct the scenario gives a similar accuracy. Based on this, in the following discussions on the accuracy of two-wall scenario reconstructions, R2 is used as reference to estimate the position of R1 in relation to surrounding walls and this is expected to give a accuracy similar to using R1 to estimate the position of R2.

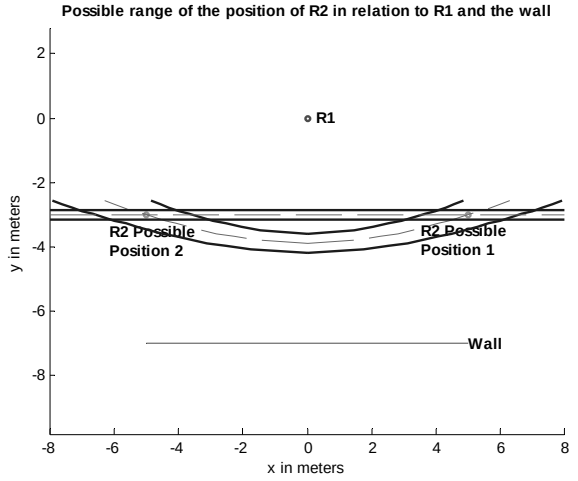

Fig. 9. Possible positions of R2 in relation to R1 and the wall after taking into account of 1ns timer error

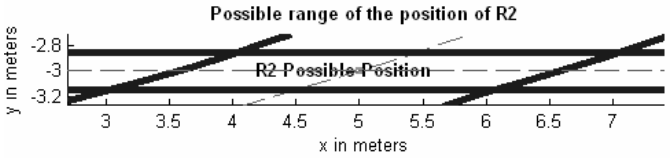

Fig. 10. Enlarged view of the region showing the actual possible positions of R2

B. Two roughly perpendicular walls

When reconstructing the two-wall scenario in Fig. 4, taking into account a very low timer resolution of 500ps, Fig. 11 shows the possible positions of R1 as two intersected parallelogram-like regions. This is derived by merging the geometry in dashed lines derived from estimating the position of R1 in relation to R2 and Wall1 with the geometry in solid lines derived from estimating the position of R1 in relation to R2 and Wall2.

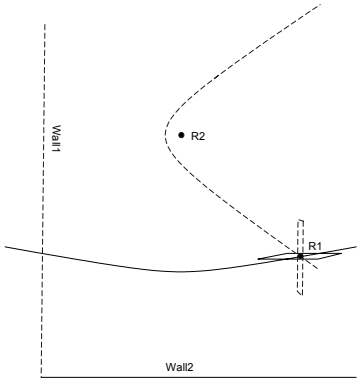

Fig. 11. Regions showing the possible positions of R1 in relation to R2 and the two surrounding walls

Fig. 12 shows the minimum possible angle between the two walls in the reconstructed scenario, while Fig. 13 shows the maximum possible angle between the two walls. It can be observed that the angles between the walls in the scenarios shown in Fig. 12 and Fig. 13 are quite different. For comparison purposes, effects of timer resolution in reconstructing environments comprising two parallel walls are investigated.

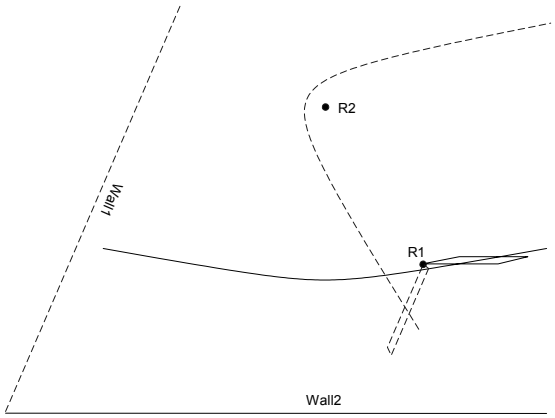

Fig. 12. Reconstructed scenario showing the minimum possible angle between the two walls

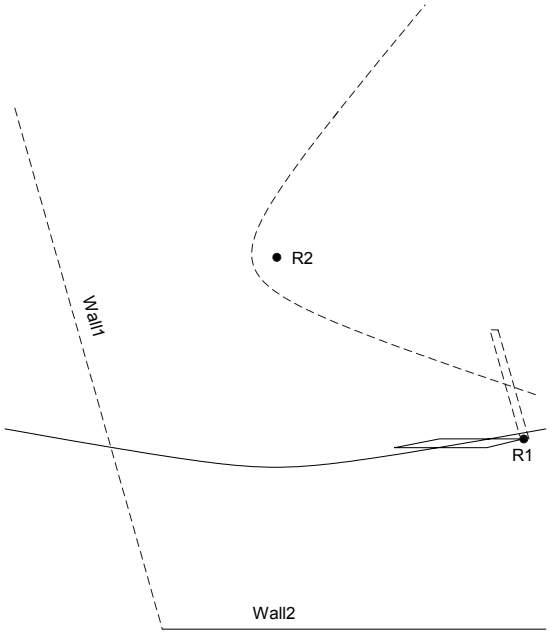

Fig. 13. Reconstructed scenario showing the maximum possible angle between the two walls

C. *Two roughly parallel walls*

Fig. 15 and Fig. 16 show the two worst cases when reconstructing the scenario shown in Fig. 14 with a timer resolution of 500ps, which is the same as the timer resolution used to reconstruct the scenario in Fig. 4. The difference between the reconstructed scenarios shown in Fig. 15 and Fig. 16 is not as big as the difference between the reconstructed scenarios shown in Fig. 12 and Fig. 13. This suggests that errors in time measurements have a stronger effect on the reconstructions of indoor environments comprising roughly perpendicular walls than on the reconstructions of environments comprising roughly parallel walls.

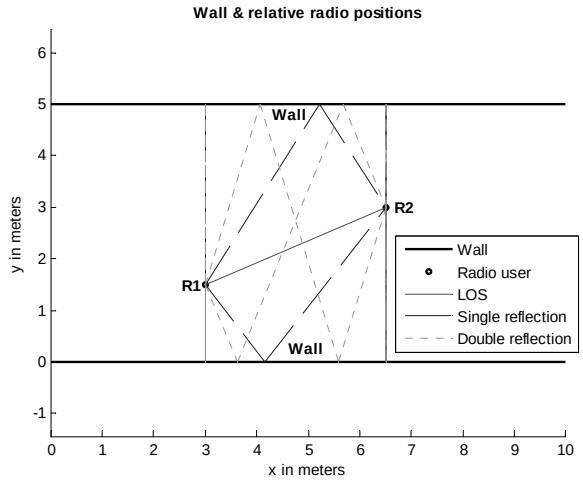

Fig. 14. Two radios communicate between two parallel walls

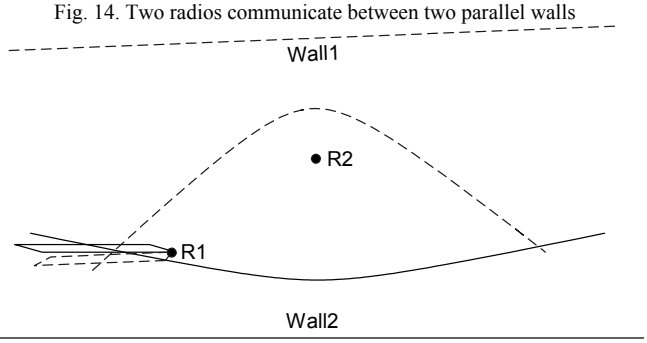

Fig. 15. Reconstructed scenario showing the maximum possible angle between the two walls when the extensions of both walls will intersect to the left

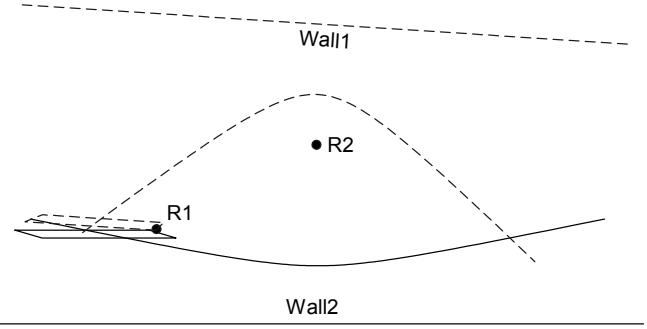

Fig. 16. Reconstructed scenario showing the maximum possible angle between the two walls when the extensions of both walls will intersect to the right

D. *Another phenomenon*

Another effect has been found when investigating the feasibility of using a single radio to reconstruct typical 2D indoor geometries. Algorithms designed for single-radio scenario reconstructions are described in [11], according to which the exact value of the angle between two walls A and B (α_{ab}) can be calculated as $\alpha_{ab} = \arccos\frac{Tab^2 - Ta^2 - Tb^2}{2 \times Ta \times Tb}$, where Tab is the TOA of the double reflection reflected by

walls A and B, Ta and Tb are the TOAs of single reflections from WallA and WallB respectively. This suggests the accuracy of reconstructed two-wall maps is related with the curve of arc cosine, as shown in Fig. 17. From this figure, it can be found that $\arccos(x)$ becomes more and more sensitive to the value of x as it decreases from 1 to 0. This is because the derivative of $\arccos(x)$, $-\frac{1}{\sqrt{1-x^2}}$, decreases as x increases. Based on this, we conclude that the best accuracy is achieved when the angle α_{ab} is close to π/2, as it is the most sensitive to the value of $\frac{TDab^2 - TSa^2 - TSb^2}{2 \times TSa \times TSb}$. On the other hand, if the calculated value of α_{ab} is close to zero, it is less accurate.

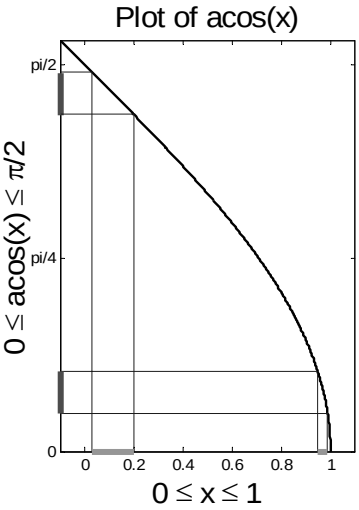

Fig. 17 The curve of arc cosine

E. A hybrid approach

Taking into account of the discussions in sections III.B and III.C, it can be concluded that, if errors in time measurements are considered, when two radios are collaborated, a greater error is possible in the results of reconstructing two roughly perpendicular walls than in the results of reconstructing two roughly parallel walls. By contrast to this, environment reconstructions using a single radio show exactly the opposite effect. Therefore, in order to achieve the best accuracy, single-radio algorithm should be used to reconstruct two roughly perpendicular walls and two-radio algorithms should be used to reconstruct two roughly parallel walls.

By improving the accuracy of two-wall geometry reconstructions, a better accuracy can be achieved in the reconstructions of more complex indoor scenarios, as these scenarios can be reconstructed by combining two-wall substructures [11,12].

IV. CONCLUSION

This paper uses 2D single-wall and two-wall sample scenarios to discuss the accuracy of environment reconstructions using the developed algorithms. The accuracies of reconstructions of two roughly perpendicular walls and reconstructions of two roughly parallel walls are compared. A hybrid approach has been addressed to achieve an improved accuracy. This approach can be applied to the reconstructions of more complex scenarios. The impulse radio mapping and positioning technique described in this paper can be used to aid indoor applications designed for location-based services or for wireless sensor networks used in disaster zones.

REFERENCE

[1] R. Want, A. Hopper, V. Falcao, and J. Gibbons, "The Active Badge Location System," *ACM Trans. Information Systems*, January 1992, vol. 10, pp. 91-102.

[2] A. Harter and A. Hopper, "A Distributed Location System for the Active Office," *IEEE Network*, January/February 1994, pp. 62-70.

[3] N.B. Priyantha, A. Chakraborty, and H. Balakrishnan, "The Cricket Location-Support System," in *Proc. 6th Ann. Int'l Conf. Mobile Computing and Networking (Mobicom 00)*, ACM Press, New York, 2000, pp. 32-43.

[4] P. Bahl and V. Padmanabhan, "RADAR: An In-Building RF-Based User Location and Tracking System," in *Proc. IEEE Infocom 2000*, IEEE CS Press, Los Alamitos, California, 2000, pp. 775-784.

[5] J. Hightower, R. Want, and G. Borriello, "*SpotON: An Indoor 3d Location Sensing Technology Based on RF Signal Strength*," UW CSE 2000-02-02, Univ. Washington, Seattle, Feb. 2000.

[6] J.Y. Lee and R.A. Scholtz, "*Ranging in dense multipath environment using an UWB radio link*", IEEE Journal on Selected Area in Communications, vol. 20, no. 9, pp. 1677-1683, December 2002.

[7] J.M. Cramer, R.A. Scholtz, and M.Z. Win, "*Evaluation of an ultra-wideband propagation channel*", IEEE Transaction on Antenna and Propagation, vol. 50, no. 5, pp. 561-570, May 2002.

[8] A.A.M. Saleh and R.A. Valenzuela, "A statistical model for indoor multipath propagation," *IEEE Journal on Selected Areas in Communications*, February 1987, pp. 123 - 137.

[9] P.F.M. Smulders, "Broadband Wireless LANs: A Feasibility Study," *PhD thesis*, Eindhoven University of Technology, Eindhoven, 1995.

[10] J. L. Richards, P. L. Jett, L. W. Fullerton, L. E. Larson and D. A. Rowe, "Precision Timing Generator Apparatus and Associated Methods," *United States Patent*, US6577691.

[11] W. Guo, N.P. Filer and R. Zetik, "Indoor Mapping and Positioning Using Impulse Radios," in *Proc. IEEE/ION Position Location and Navigation Symposium (PLANS)*, April 2006, Coronado, USA, pp. 153 - 163.

[12] W. Guo, N.P. Filer and S.K. Barton, "2D Indoor Mapping and Location-sensing Using an Impulse Radio Network," in *Proc. the 2005 IEEE International Conference on Ultra-Wideband*, September 2005, Zurich, Switzerland, pp. 296 - 301.